Development Towards Non-Invasive Monitoring of Live Animals at Longitudinal Time Points Using Synchrotron Imaging

University of Saskatchewan

Xiao Fan Ding [1], Xiaoman Duan [1], Samira Khoz [2], Daniel Chen [1,2], Ning Zhu [1,3]

[1] Division of Biomedical Engineering, [2] Department of Mechanical Engineering, [3] Canadian Light Source Inc.

Contact: xiaofan.ding@usask.ca

INTRODUCTION

Recent years have highlighted the need for imaging techniques that can non-invasively assess bioprinted materials such as hydrogel scaffolds within live physiological environments to validate their efficacy in tissue engineering and regenerative medicine [1-2]. Traditional imaging methods often fall short, lacking in image contrast [3], resolution [4], and imposing high radiation doses [5]. This study used synchrotron radiation propagation-based imaging microcomputed tomography (SR-PBI-μCT) and advanced image processing techniques for monitoring the structural dynamics of hydrogel scaffolds at longitudinal time points in the physiological environment of a rat hind limb without invasive procedures.

MATERIALS and METHODS

SR-PBI-μCT scans were performed at the BMIT 05ID-2 beamline of Canadian Light Source (CLS) using a 30 keV monochromatic beam, a 1.5 m sample-to-detector distance, a Hamamatsu AA-60 beam monitor, a 500 μm LuAG scintillator, and a Hamamatsu Orca Flash 4 camera with an effective pixel size of 13 μm. Using helical CT [6] and sparse2noise [7] scanning modes developed by our group, each scan delivered a 2.2 Gy radiation dose. Further post-image processing, as shown in Fig. 1, aimed to reduce signal interference from bone and apply the Noise2Inverse [8] technique for blind denoising, enhancing the visualization of scaffolds and tissues

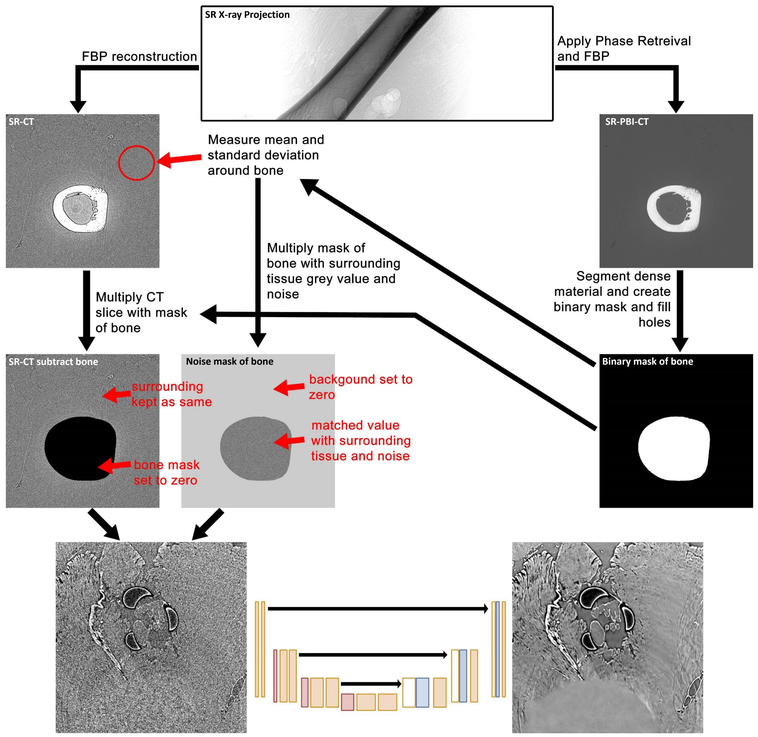

Fig 1: Image processing steps to denoise the CT reconstruction of scaffold implantation inside rat hind limb. The X-ray projection dataset was reconstructed with phase retrieval to improve contrast of the dense bone to get a bone mask, which would be used to replace the bone signal with noise from the CT reconstruction without phase retrieval. This could then be used to for blind-denoising by Noise2Inverse.

Fig 2 shows the animal model procedure which implanted hydrogel nerve repair scaffolds into the hindlimb of Sprague-Dawley rats. The animals were anesthetized using isoflurane and buprenorphine was used as the analgesic. A skin incision was made just behind the femur of the left hindlimb, and the sciatic nerve was exposed, a section of the nerve was resected, and the hydrogel scaffold within a protective polycaprolactone (PCL) stent was sutured to the two nerve stumps. After implantation, the incision was closed with wound clips. The rats were allowed to recover with the hydrogel scaffold for 2- and 4-days before euthanasia by transcardial perfusion by formalin for fixed tissue and phosphate-buffered saline (PBS) for fresh tissue. Both the operated hindlimb containing the hydrogel scaffold and the unoperated leg were removed; a scaffold was also implanted in the unoperated leg to simulate baseline conditions at 0 days. The experiment was performed with approval of the University of Saskatchewan Committee on Animal Care and Supply.

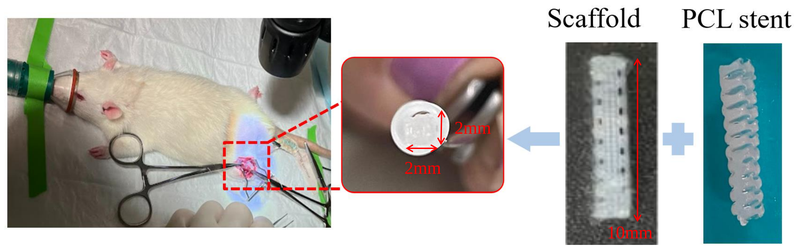

Fig 2: Animal model where a section of 2 mm x 2 mm x 10 mm hydrogel scaffold was sutured to rat sciatic nerve.

RESULTS

Hydrogel scaffolds at time points of 0-, 2-, and 4-days post-surgery were imaged through SR-PBI-μCT and shown in Fig 3. This captured the changes in scaffold structure and density both in the fresh tissue as well as the fixed tissue. This longitudinal imaging provides insights into the interactions between the implant and surrounding biological environment. Among fresh samples, at 0-days, the scaffold remains within the stent while at 2-days, the scaffold has become swollen, squeezed between the gaps of the stent, and decreased grey value. The same is seen in fixed samples. At 4-days, no noticeable scaffold structure can be seen, possibly dissolved or absorbed in the animal's body. Notably, the similarity in grey value, contrast, and visibility between fresh and fixed tissue show that the imaging techniques may be applicable towards living tissue.

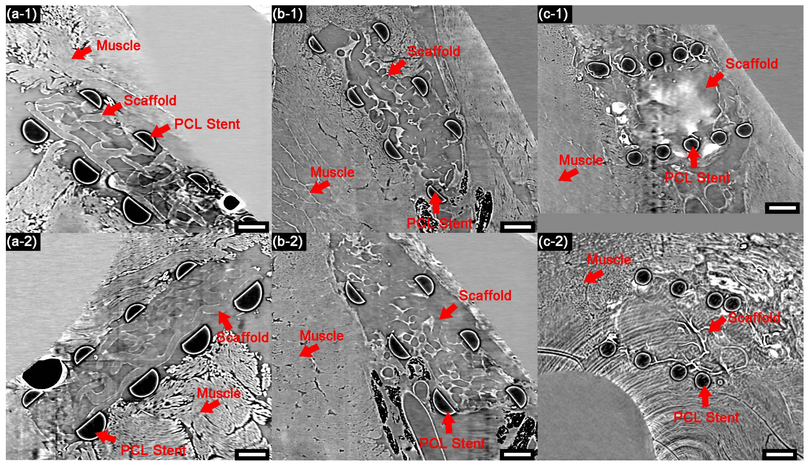

Fig 3: PBI-μCT scans of rat hindlimb samples containing hydrogel scaffold implant at longitudinal time points. (a-1) and (a-2) are fresh and fixed samples immediately after implantation (0 days). (b-1) and (b-2) are fresh and fixed samples at 2 days post-surgery. (c-1) and (c-2) are fresh and fixed samples at 4 days post-surgery. Scale bars represent 1 mm.

Fig 4 shows the response of hydrogel scaffolds to:

1) $CaCl_2$ crosslinking solution (used in strengthening hydrogel material)
2) Formalin (solution used for fixed ex vivo samples)
3) PBS (solution used for fresh ex vivo samples)
4) Culture media (to simulate interactions with bodily proteins)

Hydrogel scaffold degradation was quantitatively assessed by contrast-to-noise ratio (CNR) and volume. Notably, scaffolds in formalin and PBS showed degradation, indicated by low CNR and swelling compared to those to crosslinking solution. These observations correlate with the findings from the animal model, where scaffolds were exposed to formalin during transcardial perfusion for fixed samples and PBS for fresh samples, thereby providing a link between chemical exposure and degradation. Furthermore, the culture media, which simulates how the hydrogel scaffold reacts inside the body, also exhibits similar degradation. The 3D renders show the volume of the hydrogel scaffold in each solution. These models were segmented using the EdgeView strategy developed in this lab [9,10,11] enhancing the understanding of physical alterations in scaffold structure in response to each solution. The swelling corresponds to a decrease in scaffold density and CNR. By measuring the volume of each scaffold, we can quantitatively assess the impact of different solutions on the scaffold's mechanical integrity.

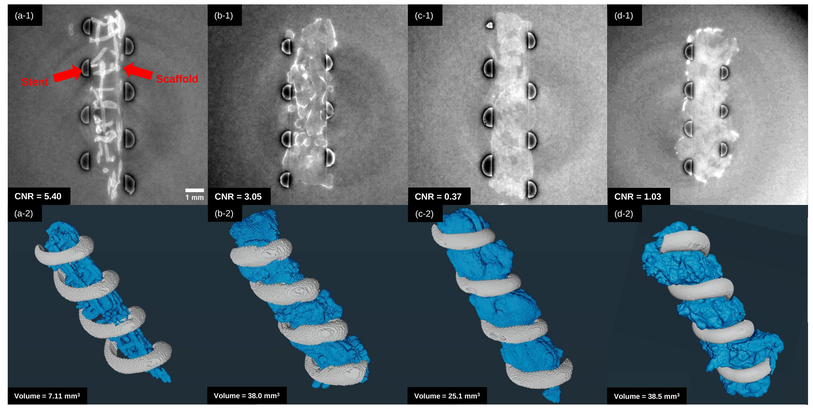

Fig 4: The condition of hydrogel scaffolds designed for implantation in different solutions: (a-1) and (a-2) $CaCl_2$ crosslinking solution, (b-1) and (b-2) formalin, (c-1) and (c-2) PBS, (d-1) and (d-2) culture media. The scale bar in the top row represents 1 mm for all images. The bottom row shows 3D models of segmented hydrogel scaffolds (blue) and stent (grey) show the changes in volume. The same printed scaffold design was subject to each solution.

DISCUSSION and CONCLUSION

The current imaging system and image processing steps are advantageous for providing high contrast, low noise, and low dose imaging. However, with new advances in imaging detectors, there's also a need to continually fine tune our algorithms to new data. The BMIT beamline obtained a new detector in 2024 which can acquire images more efficiently and at an effective pixel size of 5 μm. This is a significant improvement to the 13 μm detector that allows for visualization of pores inside bones, muscle fibers, and adipose tissue that was previously difficult as shown in Fig 5.

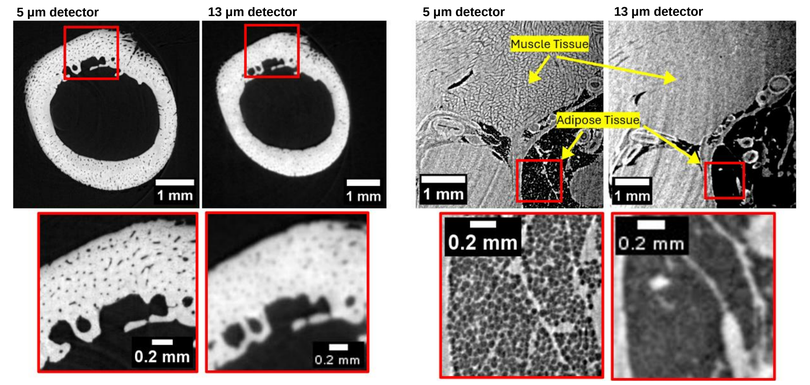

Fig 5: Comparison between a new 5 μm pixel detector system and a 13 μm detector system. The newer detector provides greater detail of inside bones (left) and surrounding tissues (right).

This study demonstrates the use of SR-PBI-μCT techniques for non-destructive analysis of hydrogel scaffolds in animal tissue at longitudinal time points. This provides valuable insights into the challenges of scaffold degradation and the dynamic interactions within biological environments. The findings also emphasize the need for enhancements in scaffold design as imaging technologies improve and image processing algorithms adapt to new data as we move towards live animal monitoring at longitudinal time points.

REFERENCES

[1] Ning et al. *ACS Appl Mater Interfaces.* 2021
[2] Duan et al. *Tissue Eng Part C Methods.* 2021
[3] Coan et al. *Phys Med Biol.* 2010
[4] Donnelley et al. *J Synchrotron Radiat.* 2014. [5] Roman et al. *Biomaterials.* 2007
[6] Duan et al. *J Synchrotron Radiat.* 2023
[7] Duan et al. *Comput Biol Med.* 2023
[8] Hendriksen et al. *IEEE Trans Comput Imaging.* 2020
[9] Ding et al. *Biofabrication 2023*
[10] github.com/xfding57/EdgeView-Segmentation
[11] Ding et al. *J Med Imaging. Submitted*

ACKNOWLEDGEMENTS

NSERC CRSNG
INSPIRE
University of Saskatchewan
Canadian Light Source
Centre canadien de rayonnement synchrotron
Light exploring life BMIT